



Water disinfection using durable ceramic filter coated with silver nanoparticles synthesized using actinomycetes

Karam Rabee Wafy¹ · Eslam Ibrahim El-Aswar¹ · Walaa Salah El-din Mohamed¹ · Sabha Mahmoud El-Sabbagh²

Received: 12 December 2022 / Accepted: 2 May 2023 / Published online: 27 May 2023
© The Author(s) 2023

Abstract

Contamination with pathogens degrades water quality and is a major cause of many waterborne diseases. The aim of this research is to reduce the global disease burden by presenting an efficient, durable, and low-cost ceramic filter impregnated with actinomycetes-mediated silver nanoparticles (AgNPs) for water disinfection in rural areas. This marks the first report on the simultaneous biosynthesis of AgNPs utilizing cell-free supernatants obtained from terrestrial actinomycetes. An easy and efficient method was used to impregnate AgNPs onto a ceramic filter using 3-aminopropyltriethoxysilane (APTES). The APTES linker is anchored to the ceramic surface through Si–O–Si bridges, while the terminal amino groups coordinate with AgNPs. Notably, the observed inhibition zone around the filter with AgNPs was ~ 18 mm, suggesting that the silver ions were responsible for the antibacterial activity. After 30 min of sonication, only insignificant traces of AgNPs were released from the filter, making it stable for long-term antibacterial activity when treating water. According to the laboratory simulation experiments, the untreated filter can reject about 99% of spiked bacteria, while the antibacterial efficiency of the filter coated with AgNPs was 100% due to the synergistic effect between filtration and disinfection with AgNPs. In addition, the average concentration of dissolved silver in the outlet water of the ultrafiltration system during three months was 33.7 µg/L, far below the permissible limit (100 µg/L) for drinking water. Overall, this work offers a suitable and affordable water treatment strategy for low-income, isolated, and rural societies in developing countries.

Keywords Actinomycetes · AgNPs · Ceramic filter · Antibacterial activity · Water treatment

Introduction

Water is a crucial commodity for human civilization and an invaluable resource for a wide range of activities, from industry to agriculture to the medical sector. Nevertheless, the lack of safe drinking water remains a global concern, particularly in developing countries (He et al. 2019; Abdelfattah et al. 2022; Nassar et al. 2023). Southeast Asia, the

Middle East, and North Africa are dealing with significant problems in meeting the growing demand for clean and safe water due to the global industrialization, urbanization, rapid population growth, climate change, and high water quality demands (El-Aswar et al. 2022; Abdelfattah et al. 2023; Sanad et al. 2023). According to the World Health Organization (WHO), over 2 billion people lack access to safe drinking water, and by 2025, half of the world's population will live in regions with severe water scarcity (Mekonnen and Hoekstra 2016). A statistical analysis of WHO indicated that roughly 80% of diseases are caused by polluted drinking water (Liu et al. 2017; Verdin 2019). Waterborne diseases including diarrhea, cholera, and gastrointestinal diseases are caused by the contamination of water bodies by numerous bacteria, viruses, and protozoa, and this is a major problem on a global scale. Safe drinking water should be free of fecal and total coliforms (Pérez-Vidal et al. 2019; El-Aswar et al. 2020).

Karam Rabee Wafy and Eslam Ibrahim El-Aswar have contributed equally to this work and should be considered as co-first authors.

✉ Eslam Ibrahim El-Aswar
eslam_desoke@nwrc.gov.eg

¹ Central Laboratories for Environmental Quality Monitoring (CLEQM), National Water Research Center (NWRC), P.O. Box 13621, El-Kanater, Qalyubiyah, Egypt

² Department of Botany and Microbiology, Faculty of Sciences, Menoufia University, Shebin El-Kom 32512, Menoufia, Egypt

There are various disinfection methods used to eliminate microbial diseases, such as chlorine, chlorine derivatives, ozone, and ultraviolet disinfection, but each method has its limitations (Yang et al. 2019). When chlorine is used for disinfection purposes, it produces carcinogenic disinfection byproducts (DBPs) such as trihalomethanes. The DBPs are formed when chlorine reacts with natural organic matter in water (NOM) (Mazhar et al. 2020). The main drawbacks of UV-based water disinfection systems are their relatively high cost and the required energy source. Additionally, harmful DBPs are formed during UV treatment if NOM is present (Rauch et al. 2022). Ozonation is a more complex technology than other disinfection strategies and is not cost-effective for poor quality water due to the required corrosion-resistant material (Morrison et al. 2022). Membranes have also been used for disinfection purposes, but biofouling and the high cost of membrane modules restrict their application. Therefore, it is crucial to reevaluate traditional disinfection methods and develop more innovative and economical methods for obtaining clean drinking water (Goswami and Pugazhenti 2020). Recently, ceramic membranes have gained widespread attention due to their technical advantages such as longer lifetime, higher mechanical, thermal, and chemical stability, high flow rates at low pressure, well-defined pore size distribution, and good hydrophilicity (Samaei et al. 2018; He et al. 2019). However, there are still challenges in using ceramic filters since they can only block bacteria without killing them. Hence, bacteria strongly adhere to the surface and form biofilms, which makes the ceramic membrane a potential source of contamination. Additionally, this biofilm is resistant to antimicrobial agents; thus, it cannot be removed by conventional methods (Fu et al. 2016; Li et al. 2017). To address this issue, the ceramic membrane should have antibacterial properties to prevent biofilm formation. This could be achieved by coating the surface with antimicrobial agents.

Recent developments in nanomaterials hold promise for the production of next-generation water disinfection systems (Santhosh et al. 2016; Gur et al. 2022). However, physically and chemically synthesizing nanostructures can be costly and time-consuming, making it unsuitable for mass production (Kolahalam et al. 2019; Mahmoud 2020). Moreover, chemical processes rely on noxious chemicals and solvents that are not environmentally friendly and can produce toxic byproducts and intermediates (Tulinski and Jurczyk 2017; Pottathara et al. 2019). Using biological processes is a cost-effective, sustainable, and eco-friendly alternative since the production of nanomaterials can significantly reduce the utilization of harmful compounds (El-Aswar et al. 2019; Liang et al. 2022). In biosynthesis, nanomaterials are produced from various natural sources such as plant extracts, fungi, bacteria, algae, and biomolecules under physico-chemical conditions (El-Kemary 2016; Karimi et al. 2023).

Actinomycetes, a distinct group of filamentous gram-positive bacteria with a cosmopolitan distribution, thrive even in extreme conditions such as high temperatures, extreme pH, or water stress (Aparicio et al. 2018; Gohain et al. 2020). Actinomycetes are a treasure trove of various secondary metabolites that can promote the biosynthesis of various nanomaterials and act as bioreducing and stabilizing agents (Salwan and Sharma 2020; Jose et al. 2021).

Silver has long been recognized as an effective antibacterial agent due to its ability to inhibit and kill bacteria without producing harmful chemical products. Nevertheless, the cost and low ion release rate of silver limit its use in bulk applications for household or industrial purposes (Ngoc Dung et al. 2019; Peng et al. 2020). However, silver nanoparticles (AgNPs) have an impressively strong antibacterial effect compared to bulk silver due to their large surface area, even at low doses. Nevertheless, due to the possibility of toxic bioaccumulation and difficulties in their recovery from the environment or their possible aggregation during storage, the use of AgNPs is limited (He et al. 2019; Göll et al. 2020). To overcome these control, health, and environmental issues in the application of nanomaterials, scientists have proposed attaching, incorporating, or impregnating nanostructures onto more durable and stable substrates. The simplest impregnation technique involves immersing the substrate (ceramic filter) in the solution of an antimicrobial agent (AgNPs). However, despite its simplicity, this approach has significant drawbacks, as the coated AgNPs are rapidly leached during the filtration process due to weak van der Waals interactions. This leaching significantly compromises the antibacterial effectiveness of the ceramic filter (Ewis et al. 2021; Mehta et al. 2021). As a result, a new practical and efficient procedure has been proposed to prevent leaching of AgNPs by anchoring the nanoparticles on the activated and functionalized surface of the ceramic filter. By depositing 3-aminopropyltriethoxysilane (APTES), an aminosilane, on the surface of the ceramic membrane and binding it by siloxane (Si–O–Si) condensation, the nanoparticles are coordinated with the anchored amino groups via N–Ag bonding, which ensures high stability and nanoparticle fixation and prevents their detachment (Lv et al. 2009; Ehdiaie et al. 2014; Ngoc Dung et al. 2019).

The aim of this study was to develop a commercial ceramic filter with high antibiofouling properties by coupling biogenic AgNPs to its surface using aminosilane. We compared the efficacy of this modified ceramic filter to that of unmodified filters in the biological pretreatment stage during water disinfection. The production of AgNPs was achieved using cell-free supernatants derived from terrestrial actinomycetes cultures, which is a green, facile, and sustainable approach. To our knowledge, this is the first report on this method of AgNPs production. The durability and reusability of the developed composite were tested

by examining the strength of the interconnecting bridges formed between AgNPs and the surface of the ceramic filter. This biogenic AgNPs-decorated ceramic filter presents a promising and affordable water treatment strategy, especially in rural societies.

Materials and methods

Collection and isolation of actinomycetes

At a depth of 15–20 cm, soil samples were collected in sterile plastic bags and transferred to the laboratory. Actinomycetes were isolated from the soil using physical treatment. Following drying at 105 °C for 45 min, nearly 1 g of each sample was serially diluted 5–10 times, and 100 µL of each dilution was spread on starch agar media plates (3 g/L beef extract, 10 g/L starch, 15 g/L agar, pH 7.2 ± 0.1). The plates were incubated at 27 °C for 7–14 days, subcultured, and pure colonies were preserved in the refrigerator for further use.

Biosynthesis of AgNPs using cell-free supernatant

Actinomycetes species were cultured using starch broth media in an orbital shaker incubator at 30 °C with agitation at 120 rpm. After incubating for 4 days, the culture was centrifuged at 4500 rpm for 30 min to remove the biomass. A mixture of 10 mL of cell-free filtrate and 250 mL of 5 mM silver nitrate aqueous solution (CARLO ERBA Reagents) was agitated in the dark at 150 rpm and 28 °C on a shaker to obtain a dark brown colloidal suspension of AgNPs. The suspension was then transferred to 25-mL sealed vials to be embedded onto the ceramic filter surface.

Identification of the best isolates by 16S rRNA sequencing

The actinomycetes isolate with the highest yield of silver nanoparticles was selected for 16S rRNA sequencing. It was inoculated into starch casein broth and incubated at 28 °C for 7 days. Genomic DNA was extracted using the Quick-DNA Miniprep Plus Kit (Zymo Research Corp., USA). The 16S rRNA universal primers gene fragment was amplified by polymerase chain reaction (PCR) using purified genomic DNA as the template, a forward primer (5'-GTTGGTGAGGTAACGGCTCA-3'), and a reverse primer (5'-CCACCTTCCTCCGAGTTGAC-3'). The PCR reaction was performed under the following conditions: initial denaturation at 94 °C for 6 min, 35 amplification cycles of 94 °C for 45 s, 56 °C for 45 s, and 72 °C for 1 min, and a final extension at 72 °C for 5 min. PCR products were detected and visualized using agarose gel electrophoresis and UV fluorescence. Sequencing was performed using the primers mentioned above on an automated sequencer. The

16S rRNA sequence was compared for similarity with reference species sequences using the BLAST function available at <https://www.ncbi.nlm.nih.gov/nucore/OK446664.1>, and phylogenetic analysis of these sequences was performed using the neighbor-joining method in MEGA version 11.

Modification of ceramic filter with AgNPs

The ceramic filters used (British Berkefeld Co., England) were primarily manufactured from diatomite and clay, with dimensions of 2.25 × 4.5 × 11.75 inches. Prior to impregnating AgNPs, the ceramic filters were activated by being dipped in a boiling piranha solution (1:3 v/v, 30% H₂O₂/98% H₂SO₄) for 15 min, washed with deionized water, and then soaked in a 2% ethanol solution of APTES (Sigma-Aldrich) (pH = 3.5–5.5) at room temperature for 45 min to introduce amino groups onto the activated filter surface. To ensure full condensation of the APTES molecules, the resulting filter was treated in a vacuum oven for 3 h at 100 °C. Subsequently, the APTES filter was immersed in a solution of AgNPs overnight, washed with ethanol to eliminate all unbound AgNPs, and finally air-dried. Figure 1 illustrates the steps involved in AgNPs biosynthesis and their fixation on the ceramic filter. To inspect coating integrity of the AgNPs, three samples of the modified filters were subjected to ultrasonic irradiation for 30 min while being dipped in water, and the water was quantified using ICP-MS (Inductively Coupled Plasma Mass Spectrometer, ELAN DRCe, PerkinElmer).

Characterization of the prepared material

The biosynthesis of AgNPs was examined by recording the UV–visible spectrum of the reaction at different timepoints using a UV–Vis spectrophotometer (Hach DR 3900 Spectrophotometer). The size of the biosynthesized AgNPs was determined using TEM (JEM-2100 electronic microscope, JEOL, Japan), and their crystal structure was identified using X-ray diffractometer (XRD, D8, Bruker, Germany). Fourier transform infrared (FTIR) spectra of both the APTES solution and APTES-cross-linked AgNPs were detected using a Thermo Fisher Nicolet iS50 FTIR Spectrometer. SEM (Quanta FEG 250, USA) equipped with energy-dispersive X-ray (EDX) spectroscopy was used to examine the morphological features of both the pristine ceramic filter and the AgNPs-decorated ceramic filter.

Microbiological experiments

Zone of inhibition test

The antibacterial activity of AgNPs was evaluated using the agar well diffusion method for modified Kirby-Bauer

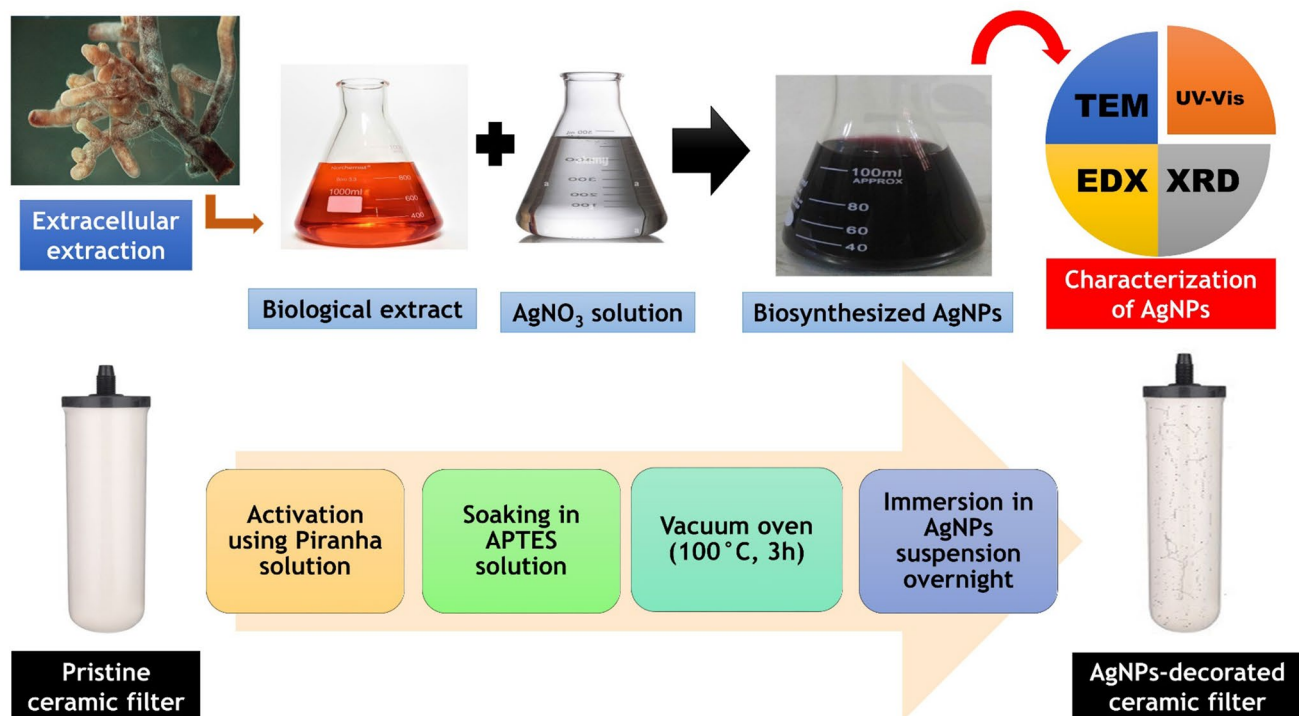


Fig. 1 Schematic diagram illustrates the steps of the biosynthesis of AgNPs and their fixation on the ceramic filter

technique. Nutrient agar plates were swabbed with different reference bacterial strains, including *E. coli* MTCC 739, *Pseudomonas aeruginosa* MTCC 2453, *Staphylococcus aureus* MTCC 96, and *Bacillus subtilis* MTCC 736. AgNPs with varying concentrations (10, 25, and 50 $\mu\text{g}/\text{mL}$) were loaded into the wells in the plates, and the plates were subsequently incubated at 37 °C for 24 h. Any inhibition zone was indicative of antibacterial activity, and the diameter of the zone was measured to the millimeter. Sterile distilled water was used as the negative control, while ceftriaxone served as the positive control.

Flow test

Comparatively, the antibacterial properties of the ceramic filter sans AgNPs were assessed against AgNPs-coated ceramic filters. Laboratory simulations using a mimetic water filter were employed. The filters were subjected to 6 L of pure water containing 4 strains of bacteria commonly used as a reference. The water was flowed at a rate of 0.1 L/min and then collected in sterilized conical flasks. To quantify the bacterial count, 100 μL of the filtered sample was collected and incubated for 24 h at 37 °C via the pour plate method. The percentage of bacteria that got filtered out from the overall count was taken as a reference to determine the antibacterial efficiency of the filters.

Dissolution of AgNPs

To assess the stability of AgNPs on the membrane surface and to determine their release into the solution, an ultrafiltration system was used to conduct a three-month test on the modified filter as a pretreatment unit. Subsequently, the permeate was sampled daily and analyzed using ICP-MS to quantify the AgNPs release.

Results and discussion

Actinomycetes characterization

In this study, 60 soil isolates of actinomycetes species were employed for AgNP biosynthesis. *Streptomyces parvulus* strain K2 was determined to be the best isolate with a high AgNP yield. The partial 16S rRNA sequences of the K2 strain were compared to the published representative sequences of actinomycetes from the NCBI GenBank database and were subsequently deposited in GenBank under the accession number OK446664.1 (Fig. S1).

Characterization of biosynthesized AgNPs

The synthesis of AgNPs was tracked primarily by the change in color of the culture filtrate from light yellow to dark

brown after 48 h of incubation, which was induced by a shift in surface plasmon resonance caused by metal particle absorption. The UV–visible spectra of the AgNPs showed maximum absorption at 420 nm (Fig. S2), falling within the typical absorption band of 410–440 nm reported for AgNPs (El-Aswar et al. 2020). Secondary metabolites in the cell-free supernatant played an influential role in the bioreduction and stabilization of AgNPs. This situation suggests that silver cations in the solution were bioreduced to metallic silver by extracted secondary metabolites (Korkmaz et al. 2020).

The mono-dispersed AgNPs were nearly spherical with a diameter of 5–45 nm (Fig. 2a and b). The biosynthesis of AgNPs was confirmed by an obvious peak around 3.0 keV in the EDX analysis (Fig. 2c). The lack of nitrogen indicated the reduction of AgNO₃ to AgNPs (Vijayabharathi et al. 2018). In the XRD analysis, four intense peaks appeared in the whole spectrum at 2θ values of 38.25°, 46.37°, 64.60°, and 77.62°, corresponding to (111), (200), (220), and (311) planes of silver, respectively (Fig. 2d). The obtained AgNPs were pure without any additional peaks for impurities. Indexing of the XRD peaks detected to a face-centered cubic structure of Ag from the available literature (JCPDS, File No. 4-0783 and 84-0713) further confirmed the synthesis of AgNPs.

Deposition of AgNPs onto a ceramic filter

The outer surface of the ceramic filter turned from white to dusky white after impregnation with AgNPs, as shown in Fig. S3. Additionally, the integrity of the AgNP coating was high, as ICP-MS only detected negligible traces of AgNPs in ultrasonically irradiated water. In contrast, samples of ceramic filters containing AgNPs but without the coupling agent APTES lost their AgNPs after ultrasonic irradiation, indicating the important role of APTES in achieving high durability with the modified ceramic filter. Scanning electron micrographs revealed successful deposition of AgNPs on the ceramic filter surface (Fig. 3a and b). Furthermore, EDX analysis verified the presence of AgNPs on the filter surface. Notably, the blank ceramic filter's EDX spectrum showed no signal for AgNPs (Fig. 3c), while that of the AgNP-decorated ceramic filter showed high peaks of elemental silver (Fig. 3d). The FTIR studies confirmed the connection between AgNPs and APTES molecules. The FTIR spectra of both the APTES solution and APTES-cross-linked AgNPs are displayed in Fig. 4. The APTES solution showed two weak bands at 3360 cm⁻¹ and 3441 cm⁻¹ (Fig. 4a), corresponding to the N–H stretches of primary amines. After development of N–Ag coordinated bonds in APTES-cross-linked AgNPs, these broad bands slightly shifted and their intensity improved (Fig. 4b). This suggests an interaction between AgNPs and the amine nitrogen of APTES molecules (Lin et al. 2013; Zhi et al. 2015). The

broad characteristic bands observed at 2967–2882 cm⁻¹ correspond to –CH₂ group stretching vibrations. Deformation of the –CH group caused by the interaction between AgNPs and the amine groups at the carbon chain's top results in a red shift and an increase in peak intensity (Freire et al. 2019). These observations confirmed the linkage between the biosynthesized AgNPs and the amine nitrogen atoms of APTES. Nonetheless, obtaining a favorable FTIR spectrum of the modified porous ceramic powder to prove the link between APTES and the ceramic surface was difficult.

Based on our observations, we proposed a mechanism for fixing AgNPs onto the ceramic filter surface (Fig. 5). First, APTES molecules' ethoxy groups are hydrolyzed in water, forming hydroxyl silane. Next, a condensation reaction occurs between hydrolyzed APTES molecules and ceramic filter surface hydroxyl groups (Si–OH), producing Si–O–Si bridges that fix the APTES molecules to the filter's surface. Since the silver atom has an empty orbital and nitrogen has a lone pair of electrons, the terminal –NH₂ group of APTES can then coordinate with silver atoms (Lv et al. 2009; Trang et al. 2018), creating an AgNP-decorated ceramic filter composite.

Microbiological results

We evaluated the antibacterial effectiveness of AgNPs against pathogenic bacteria (Fig. 6). Table 1 depicts the zones of inhibition produced by various concentrations (10, 25, 50 µg/mL) of the biosynthesized AgNPs. The negative control did not exhibit any inhibition zones, confirming that the distilled water (DW) and actinomycetes culture supernatant offered no activity against the bacteria. The biosynthesized AgNPs demonstrated maximum antibacterial efficacy against *E. coli*, *P. aeruginosa*, *S. aureus*, and *B. subtilis*. Across concentrations, the antibacterial efficacy was directly proportional to the AgNPs' concentration due to an increase in silver ion concentrations (Tiri et al. 2022). Results show better gram-positive bacterial inhibition compared to gram-negative bacteria. The antibacterial impact of 50 µg/mL AgNPs was comparable to the positive control's 10 µg/mL ceftriaxone. An array of studies on AgNPs corroborate our findings (Huq et al. 2022; Karimi et al. 2023). Previous research found that biogenic AgNPs produced using *Mimusops elengi* had bactericidal effects on tested bacteria, including *Listeria innocua*, *Enterococcus durans*, *Klebsiella pneumoniae*, *Salmonella enteritidis*, *S. epidermidis*, *B. subtilis*, and *E. coli*, at a concentration of 625 µg/mL (Korkmaz et al. 2020). Additionally, there was no evident bacterial growth on the AgNP-modified ceramic filter, but the untreated ceramic filter allowed bacterial growth (Fig. 7). The inhibited zone's presence suggests that the antibacterial action resulted from the released silver ions and not the AgNPs themselves.

Fig. 2 TEM images (a and b), EDX spectrum and the table inset the percentage of elements (c), and XRD (d) of biosynthesized AgNPs

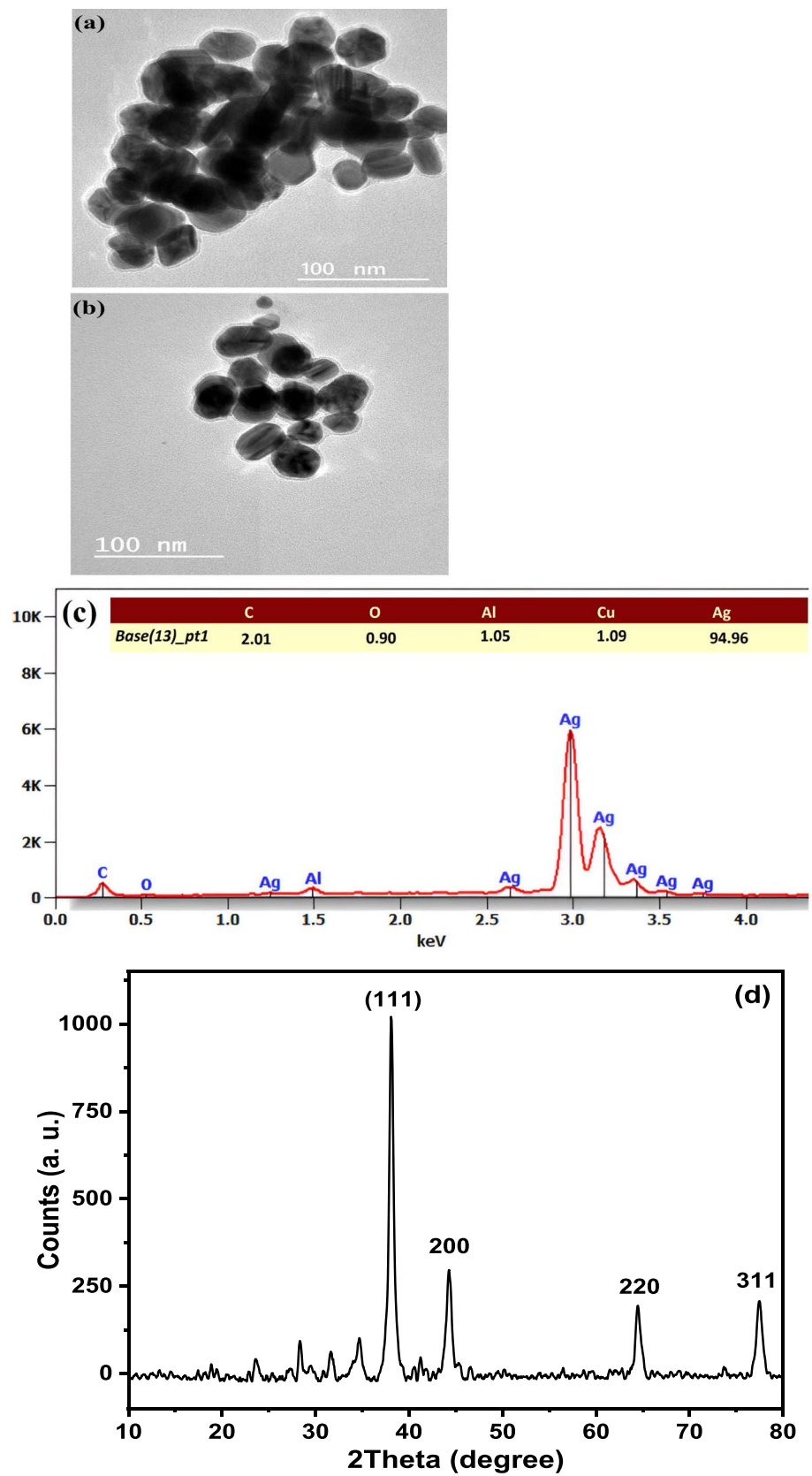
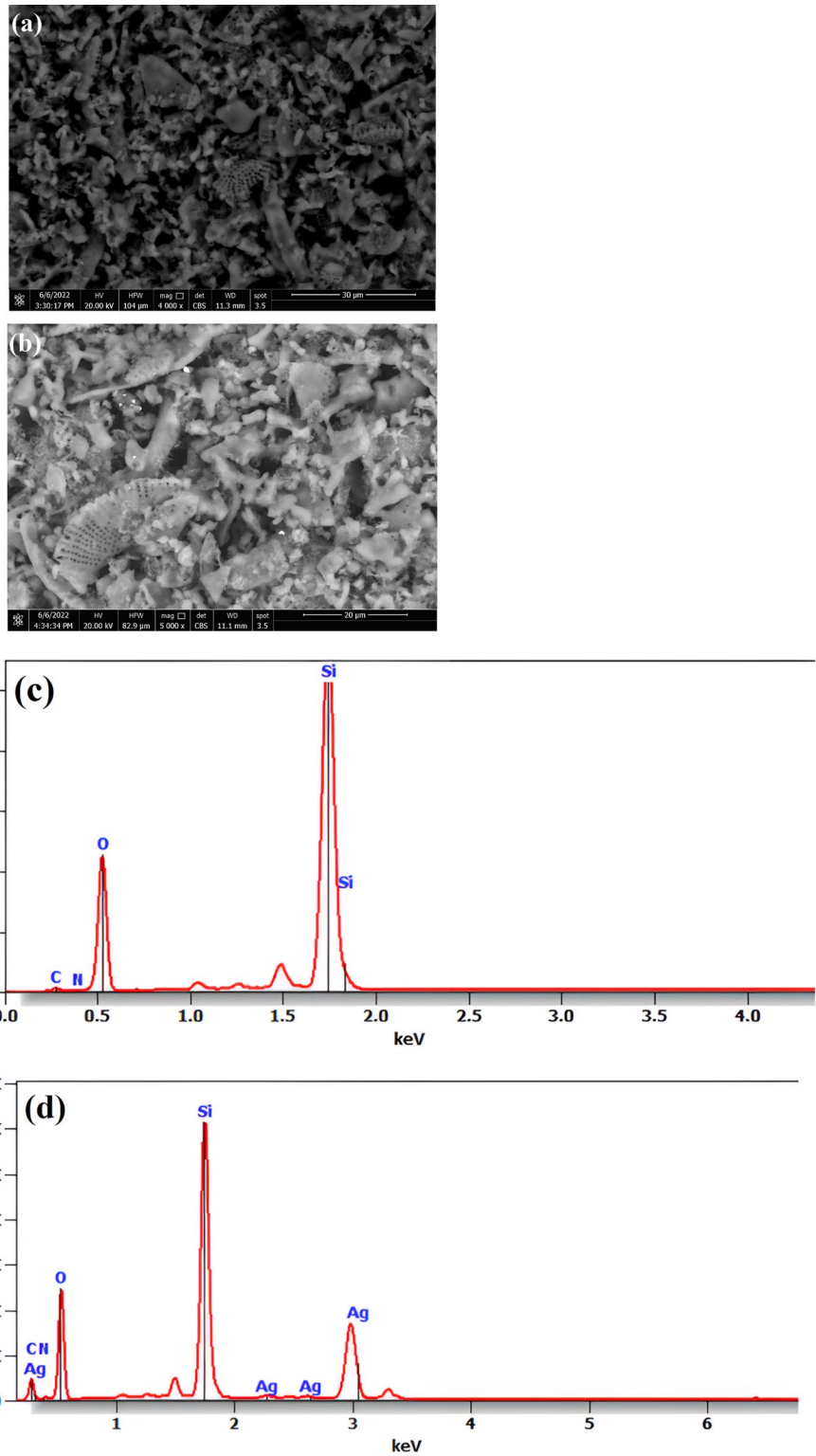


Fig. 3 **a** SEM images of pristine ceramic filter, **b** AgNPs-decorated filter, **c** EDX of blank and **(d)** modified ceramic filter



As per Table S1 flow test results, the pristine ceramic filter's bacteria elimination capacity was lower than the AgNPs-modified filter. Although the untreated filter boasts the ability to remove nearly 99% of spiked bacteria, biogenic AgNP modification of the filter increased removal efficacy

to 100%, implying that there were no bacteria detected following filtration via the ceramic filter enhanced with AgNPs. The porous architecture for the original and modified ceramic filters showed no significant difference. The augmented bacteria-killing effect of the AgNPs-decorated

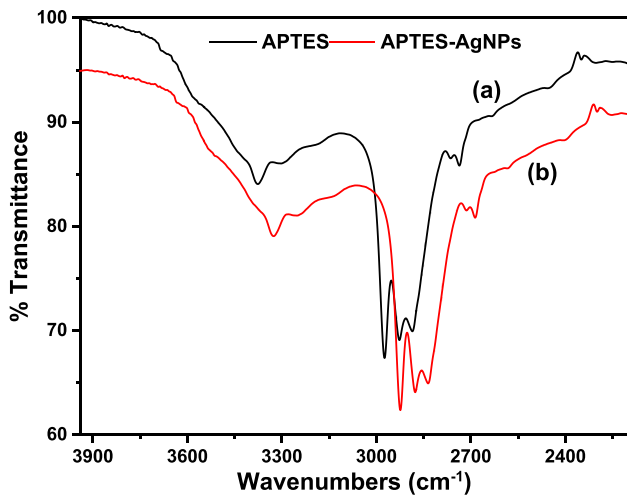


Fig. 4 FTIR spectra of pure APTES (a) and Ag nanoparticle-connected APTES (b)

filter may be due to the AgNPs (Ngoc Dung et al. 2019). Bacteria removal occurs mainly due to pore size, eliminating the majority of bacteria (99%) using non-AgNPs filter; the

minority passes through the outlet. Besides, bacteria may deposit a biofilm on the surface of the ceramic filter, emanating as a secondary source of contamination over time (Truu et al. 2022; Yu et al. 2022). Conversely, the silver released from the AgNPs-coated ceramic filter's surface may come into contact with the strain of bacteria captured via narrow pores. Due to the Ag ions interfering with cells' ability to proliferate, bacteria fail to form colonies within the filter's surface, resulting in the bactericidal effect of the filter coated in AgNPs that reaches 100%. (Ngoc Dung et al. 2019; Peng et al. 2020). Hence, all bacteria that come into contact with silver are killed, demonstrating that the filtered ceramic mechanism involves disinfection with AgNPs, possessing a synergistic effect with filtration.

Numerous theories explain AgNPs' antibacterial activity, including their potential to penetrate bacterial cell membranes and alter structure to kill the bacteria (Nouri et al. 2020; Padmavathi et al. 2022). Another hypothesis suggests that cell death may occur due to free radicals formed when Ag⁺ ions are released from the nanoparticles, causing changes in DNA replication mechanisms and inducing aberrations in size, cytoplasmic contents, and cell membranes

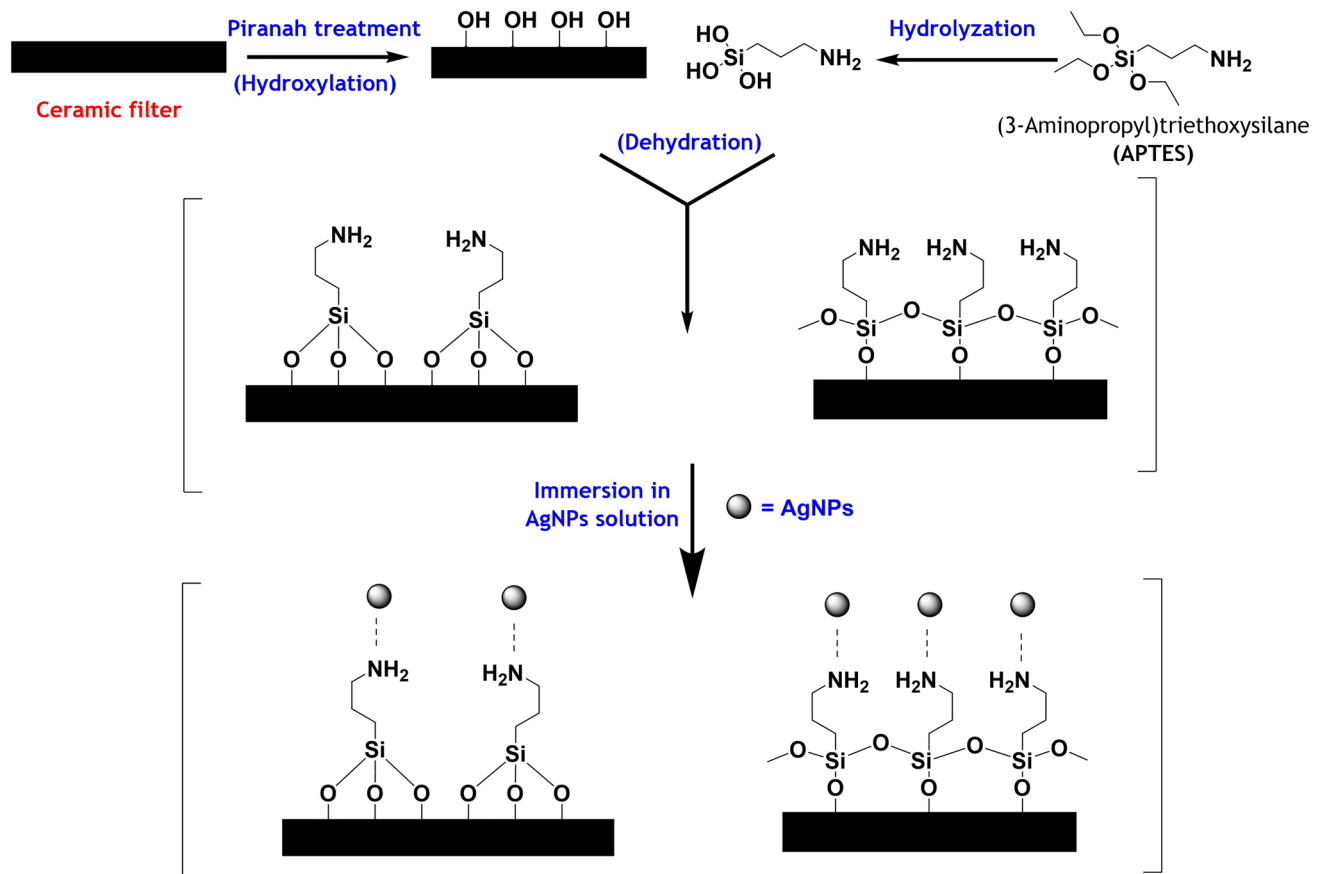


Fig. 5 Schematic diagram representing the hypothetical mechanism

Fig. 6 Antibacterial activity of biosynthesized AgNPs (A: 10 µg/mL, B: 25 µg/mL, C: 50 µg/mL, D: ceftriaxone 10 µg/mL, E: distilled water and F: supernatant)

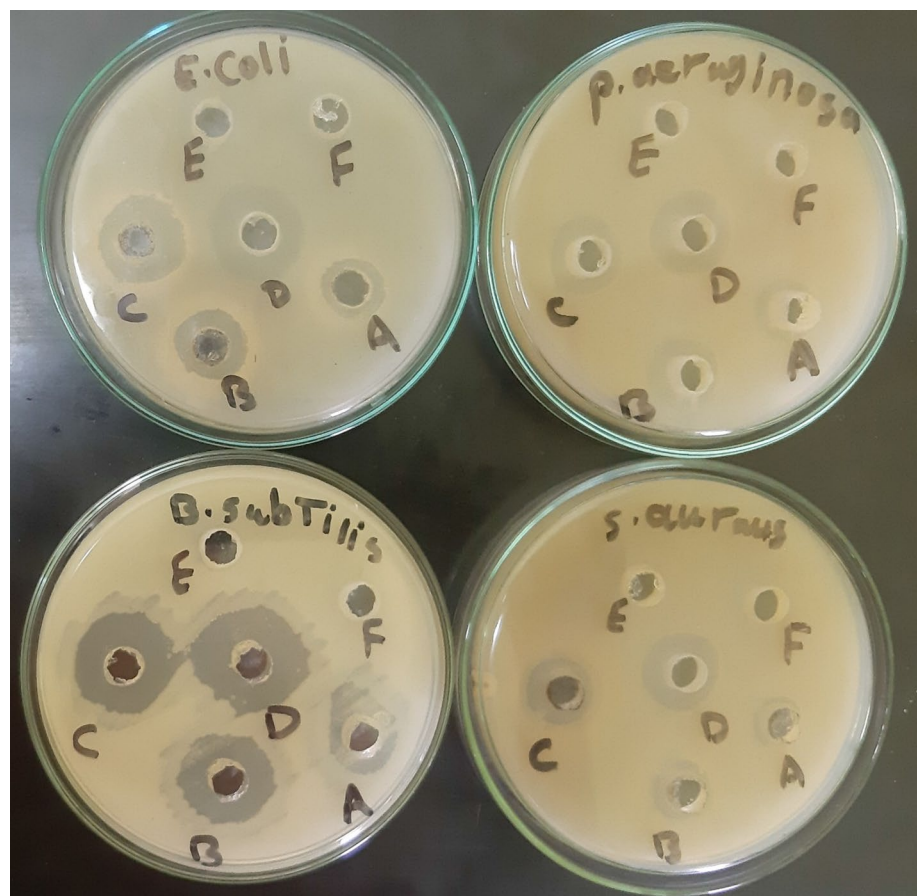


Table 1 The diameter of the inhibition zone shown by AgNPs against different microorganisms

Microorganism	Supernatant	DW	Zone of inhibition, mm			
			Ceftriaxone (10 µg/mL)	AgNPs		
				10 (µg/mL)	25 (µg/mL)	50 (µg/mL)
<i>E. coli</i>	-	-	22.6 ± 1.61	15.6 ± 1.57	18.6 ± 1.08	20.3 ± 1.43
<i>P. aeruginosa</i>	-	-	21 ± 1.38	15.3 ± 1.19	16 ± 1.59	19.3 ± 1.25
<i>S. aureus</i>	-	-	20.3 ± 1.01	12 ± 1.49	14.3 ± 1.33	17.6 ± 1.98
<i>B. subtilis</i>	-	-	25.3 ± 1.29	17.3 ± 1.19	20.6 ± 1.61	22 ± 1.05

(Tamilarasi and Meena 2020; Mani et al. 2021). In addition, the high surface area of AgNPs offers improved interaction with the bacterial membrane, which efficiently inhibits bacterial growth (Yan et al. 2018). In the present study, AgNPs were detected near the bacterial membrane (Fig. 8). Due to the electrostatic interactions between Ag⁺ ions released from the nanoparticles and the negatively charged bacterial surface, transport mechanisms and cell wall permeability become disrupted. Protein denaturation follows and the cell membrane is finally ruptured leading to cell death (El-Aswar et al. 2020; Huq et al. 2022).

In practical applications, surface water such as rivers, streams, and lakes, as well as groundwater, would experience

considerably lower bacterial density, typically less than 10³ CFU/mL. Furthermore, water undergoes sand filtration or treatment with a coagulant to remove suspended particles before disinfection and filtration. Hence, primary treatment procedures may significantly decrease bacteria counts prior to filtering with a ceramic filter (Sha’arani et al. 2019). As the experiments involved highly contaminated bacteria, the significant bactericidal effect proves that the filtered water complies with microbiological drinking water criteria.

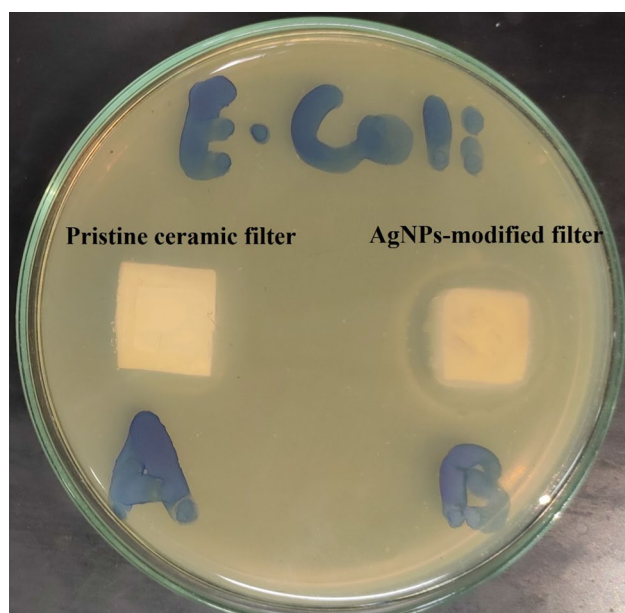


Fig. 7 Zone of inhibition of AgNPs-modified ceramic filter

Determination of the dissolution rates of AgNPs

The stability of AgNPs on ceramic filters is a vital to ensure their long-term antibacterial activity during water treatment. To examine this stability, the modified filters underwent a water bath soak under ultrasonic irradiation for 30 min. ICP-MS spectra indicated that a negligible amount of AgNPs was found in the water after ultrasonic treatment, demonstrating their high stability and efficiency coating. According to the microbial test, antibacterial activity was due to the release of Ag^+ from the modified filters. Still, excessive release of Ag^+ could lead to a loss of antibacterial activity and water pollution. Dissolution behavior was assessed using an ultrafiltration system as a pretreatment unit for 3 months. The outlet's daily dissolved Ag concentration is provided in Table S2. Over this time, the mean concentration of lost silver from the modified filter was $33.7 \mu\text{g/L}$, with a standard deviation of $3.8 \mu\text{g/L}$. The concentration is much less than the acceptable limit ($100 \mu\text{g/L}$) (Biswas and Bandyopadhyaya 2016; WHO 2021). The developed AgNPs-decorated ceramic filter meets microbiological drinking water criteria and can be commercially available for widespread use in water treatment applications, with no concerns about secondary pollution.

Conclusion

Annual health care costs related to some waterborne infections are estimated to be in the billions of dollars. To develop a new, efficient, cost-effective, and durable

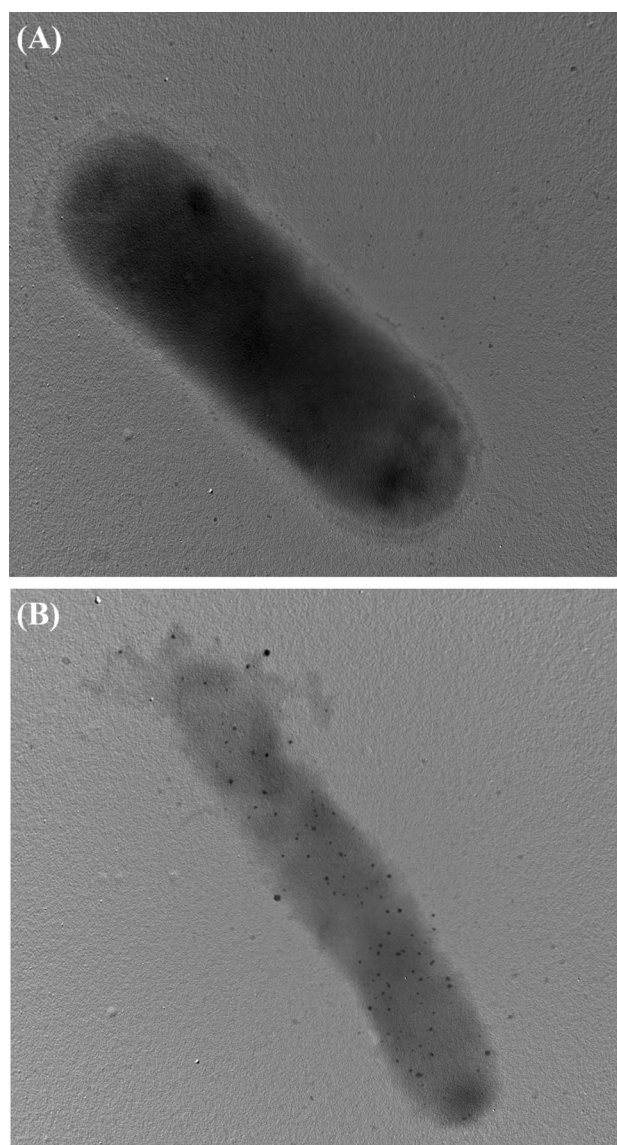


Fig. 8 TEM images of *E. coli* in the (a) absence and (b) presence of AgNPs

ceramic filter with antibiofouling properties for water treatment applications, this study aimed to overcome the limitations of most current technologies. Using an environmentally friendly and affordable method that eliminates harmful chemicals or solvents, AgNPs were biosynthesized using cell-free supernatants from cultures of actinomycetes isolated from soil. Physical characterization indicated that of the AgNPs are nearly spherical with a diameter of 5–45 nm showed a maximum UV–Vis absorption peak at 420 nm. By impregnating the biogenic AgNPs onto the ceramic filter's surface using APTES as a coupling agent, a ceramic filter crosslinked with AgNPs was developed. The coating method was efficient, and the

developed composite exhibited only slight loss of AgNPs under ultrasonic irradiation. The developed composite had strong antibacterial activity against various pathogenic bacteria. The binding between the deposited AgNPs and the amine nitrogen atoms of APTES was confirmed with FTIR studies, and EDX analysis confirmed the existence of AgNPs on the ceramic filter surface. The modified filter underwent ultrafiltration pretreatment for three months, and the amount of dissolved silver was only 33.7 µg/L. However, the efficacy of the developed composite has been studied against only four bacterial strains and may not be effective in highly contaminated water matrices. The composite's fabrication is inexpensive and simple and combined with the strong antibacterial activity, making it potentially useful for drinking water treatment in poor societies.

Supplementary Information The online version contains supplementary material available at <https://doi.org/10.1007/s13201-023-01937-y>.

Acknowledgements The authors gratefully acknowledge the National Water Research Center (NWRC) for financial support and the Central Laboratories for Environmental Quality Monitoring (CLEQM) for all the facilities they provided to carry out this work.

Author contributions KW contributed to investigation, formal analysis, methodology, writing—original draft, and writing—review and editing. EE-A contributed to conceptualization, investigation, visualization, writing—original draft, and writing—review and editing. WM contributed to resources, conceptualization, visualization, supervision, and writing—review and editing. SE-S contributed to conceptualization, resources, supervision, and validation.

Funding Open access funding provided by The Science, Technology & Innovation Funding Authority (STDF) in cooperation with The Egyptian Knowledge Bank (EKB). The authors have no relevant financial or non-financial interests to disclose.

Data availability All data generated or analyzed during this study are included in this published article (and its supplementary information files).

Declarations

Conflict of interest On behalf of all authors, the corresponding author states that there is no conflict of interest.

Open Access This article is licensed under a Creative Commons Attribution 4.0 International License, which permits use, sharing, adaptation, distribution and reproduction in any medium or format, as long as you give appropriate credit to the original author(s) and the source, provide a link to the Creative Commons licence, and indicate if changes were made. The images or other third party material in this article are included in the article's Creative Commons licence, unless indicated otherwise in a credit line to the material. If material is not included in the article's Creative Commons licence and your intended use is not permitted by statutory regulation or exceeds the permitted use, you will need to obtain permission directly from the copyright holder. To view a copy of this licence, visit <http://creativecommons.org/licenses/by/4.0/>.

References

- Abdelfattah A, Dar MA, Ramadan H et al (2022) Exploring the potential of algae in the mitigation of plastic pollution in aquatic environments. In: Abdullah N, Ahmad I, El-Sheekh M (eds) Handbook of research on algae as a sustainable solution for food, energy, and the environment. IGI Global, Hershey, pp 501–523
- Abdelfattah A, Ali SS, Ramadan H et al (2023) Microalgae-based wastewater treatment: mechanisms, challenges, recent advances, and future prospects. *Environ Sci Ecotechnol* 13:100205. <https://doi.org/10.1016/j.ese.2022.100205>
- Aparicio JD, Raimondo EE, Gil RA et al (2018) Actinobacteria consortium as an efficient biotechnological tool for mixed polluted soil reclamation: experimental factorial design for bioremediation process optimization. *J Hazard Mater* 342:408–417. <https://doi.org/10.1016/j.jhazmat.2017.08.041>
- Biswas P, Bandyopadhyaya R (2016) Water disinfection using silver nanoparticle impregnated activated carbon: Escherichia coli cell-killing in batch and continuous packed column operation over a long duration. *Water Res* 100:105–115. <https://doi.org/10.1016/j.watres.2016.04.048>
- Ehdaie B, Krause C, Smith JA (2014) Porous ceramic tablet embedded with silver nanopatches for low-cost point-of-use water purification. *Environ Sci Technol* 48:13901–13908. <https://doi.org/10.1021/es503534c>
- El-Aswar EI, Zahran MM, El-Kemary M (2019) Optical and electrochemical studies of silver nanoparticles biosynthesized by *Haplophyllum tuberculatum* extract and their antibacterial activity in wastewater treatment. *Mater Res Express*. <https://doi.org/10.1088/2053-1591/ab35ba>
- El-Aswar EI, Gaber SES, Zahran MM, Abdelaleem AH (2020) Characterization of biosynthesized silver nanoparticles by *haplophyllum tuberculatum* plant extract under microwave irradiation and detecting their antibacterial activity against some wastewater microbes. *Desalin Water Treat* 195:275–285. <https://doi.org/10.5004/dwt.2020.25876>
- El-Aswar EI, Ramadan H, Elkik H, Taha AG (2022) A comprehensive review on preparation, functionalization and recent applications of nanofiber membranes in wastewater treatment. *J Environ Manage* 301:113908. <https://doi.org/10.1016/j.jenvman.2021.113908>
- El-Kemary M (2016) *Calendula officinalis*-mediated biosynthesis of silver nanoparticles and their electrochemical and optical characterization. *Int J Electrochem Sci*. <https://doi.org/10.20964/2016.12.88>
- Ewis D, Ismail NA, Hafiz M et al (2021) Nanoparticles functionalized ceramic membranes: fabrication, surface modification, and performance. *Environ Sci Pollut Res* 28:12256–12281. <https://doi.org/10.1007/s11356-020-11847-0>
- Freire C, Nunes M, Pereira C et al (2019) Metallo(salen) complexes as versatile building blocks for the fabrication of molecular materials and devices with tuned properties. *Coord Chem Rev* 394:104–134. <https://doi.org/10.1016/j.ccr.2019.05.014>
- Fu C, Zhang X, Savino K et al (2016) Antimicrobial silver-hydroxyapatite composite coatings through two-stage electrochemical synthesis. *Surf Coat Technol* 301:13–19. <https://doi.org/10.1016/j.surfcoat.2016.03.010>
- Gohain A, Manpoong C, Saikia R, De Mandal S (2020) Chapter 9 - Actinobacteria: diversity and biotechnological applications. In: de Mandal S, Bhatt PBT-RA in MD (eds). Academic Press, pp 217–231
- Göl F, Aygün A, Seyrankaya A et al (2020) Green synthesis and characterization of *Camellia sinensis* mediated silver nanoparticles for antibacterial ceramic applications. *Mater Chem Phys* 250:123037. <https://doi.org/10.1016/j.matchemphys.2020.123037>

- Goswami KP, Pugazhenth G (2020) Credibility of polymeric and ceramic membrane filtration in the removal of bacteria and virus from water: a review. *J Environ Manage* 268:110583. <https://doi.org/10.1016/j.jenvman.2020.110583>
- Gur T, Meydan I, Seckin H et al (2022) Green synthesis, characterization and bioactivity of biogenic zinc oxide nanoparticles. *Environ Res* 204:111897. <https://doi.org/10.1016/j.envres.2021.111897>
- He Z, Lyu Z, Gu Q et al (2019) Ceramic-based membranes for water and wastewater treatment. *Colloids Surf A Physicochem Eng Asp* 578:123513. <https://doi.org/10.1016/j.colsurfa.2019.05.074>
- Huq MA, Ashrafudoulla M, Rahman MM, et al (2022) Green synthesis and potential antibacterial applications of bioactive silver nanoparticles: a review. *Polym* 14
- Jose PA, Maharshi A, Jha B (2021) Actinobacteria in natural products research: progress and prospects. *Microbiol Res* 246:126708. <https://doi.org/10.1016/j.micres.2021.126708>
- Karimi F, Elhouda Tiri RN, Aygun A et al (2023) One-step synthesized biogenic nanoparticles using *Linum usitatissimum*: application of sun-light photocatalytic, biological activity and electrochemical H₂O₂ sensor. *Environ Res* 218:114757. <https://doi.org/10.1016/j.envres.2022.114757>
- Kolahalam LA, Kasi Viswanath IV, Diwakar BS et al (2019) Review on nanomaterials: synthesis and applications. *Mater Today Proc* 18:2182–2190. <https://doi.org/10.1016/j.matpr.2019.07.371>
- Korkmaz N, Ceylan Y, Hamid A et al (2020) Biogenic silver nanoparticles synthesized via *Mimusops elengi* fruit extract, a study on antibiofilm, antibacterial, and anticancer activities. *J Drug Deliv Sci Technol* 59:101864. <https://doi.org/10.1016/j.jddst.2020.101864>
- Li X, Sotto A, Li J, Van der Bruggen B (2017) Progress and perspectives for synthesis of sustainable antifouling composite membranes containing in situ generated nanoparticles. *J Memb Sci* 524:502–528. <https://doi.org/10.1016/j.memsci.2016.11.040>
- Liang Y, Demir H, Wu Y et al (2022) Facile synthesis of biogenic palladium nanoparticles using biomass strategy and application as photocatalyst degradation for textile dye pollutants and their in-vitro antimicrobial activity. *Chemosphere* 306:135518. <https://doi.org/10.1016/j.chemosphere.2022.135518>
- Lin S, Huang R, Cheng Y et al (2013) Silver nanoparticle-alginate composite beads for point-of-use drinking water disinfection. *Water Res* 47:3959–3965. <https://doi.org/10.1016/j.watres.2012.09.005>
- Liu J, Yang H, Gosling SN et al (2017) Water scarcity assessments in the past, present, and future. *Earth's Futur* 5:545–559. <https://doi.org/10.1002/2016EF000518>
- Lv Y, Liu H, Wang Z et al (2009) Silver nanoparticle-decorated porous ceramic composite for water treatment. *J Memb Sci* 331:50–56. <https://doi.org/10.1016/j.memsci.2009.01.007>
- Mahmoud AED (2020) Nanomaterials: green synthesis for water applications. In: Kharisova OV, Martínez LMT, Kharisov BI (eds) *Handbook of nanomaterials and nanocomposites for energy and environmental applications*. Springer International Publishing, Cham, pp 1–21
- Mani M, Pavithra S, Mohanraj K et al (2021) Studies on the spectroscopic analysis of metallic silver nanoparticles (Ag NPs) using *Basella alba* leaf for the antibacterial activities. *Environ Res* 199:111274. <https://doi.org/10.1016/j.envres.2021.111274>
- Mazhar MA, Khan NA, Ahmed S et al (2020) Chlorination disinfection by-products in municipal drinking water: a review. *J Clean Prod* 273:123159. <https://doi.org/10.1016/j.jclepro.2020.123159>
- McNally A, Verdin K, Harrison L, Getirana A, Jacob J, Shukla S, Arsenault K, Peters-Lidard C, Verdin JP (2019) Acute water-scarcity monitoring for Africa. *Water* 11(10):1968. <https://doi.org/10.3390/w11101968>
- Mehta VN, Raval JB, Patel SR et al (2021) Bio-functionalized silver nanoparticles: a versatile candidate for the ceramic industry. In: Hussain CM, Thomas S (eds) *Handbook of polymer and ceramic nanotechnology*. Springer International Publishing, Cham, pp 83–98
- Mekonnen MM, Hoekstra AY (2016) Four billion people facing severe water scarcity. *Sci Adv* 2:e1500323. <https://doi.org/10.1126/sciadv.1500323>
- Morrison CM, Hogard S, Pearce R et al (2022) Ozone disinfection of waterborne pathogens and their surrogates: a critical review. *Water Res* 214:118206. <https://doi.org/10.1016/j.watres.2022.118206>
- Nassar AE, El-Aswar EI, Rizk SA et al (2023) Microwave-assisted hydrothermal preparation of magnetic hydrochar for the removal of organophosphorus insecticides from aqueous solutions. *Sep Purif Technol* 306:122569. <https://doi.org/10.1016/j.seppur.2022.122569>
- Ngoc Dung TT, Phan Thi L-A, Nam VN et al (2019) Preparation of silver nanoparticle-containing ceramic filter by in-situ reduction and application for water disinfection. *J Environ Chem Eng* 7:103176. <https://doi.org/10.1016/j.jece.2019.103176>
- Nouri A, Tavakkoli Yarak M, Lajevardi A et al (2020) Ultrasonic-assisted green synthesis of silver nanoparticles using *Mentha aquatica* leaf extract for enhanced antibacterial properties and catalytic activity. *Colloid Interface Sci Commun* 35:100252. <https://doi.org/10.1016/j.colcom.2020.100252>
- Padmavathi J, Mani M, Gokulakumar B et al (2022) A study on the antibacterial activity of silver nanoparticles derived from *Corchorus aestuans* leaves and their characterization. *Chem Phys Lett* 805:139952. <https://doi.org/10.1016/j.cplett.2022.139952>
- Peng S, Chen Y, Jin X et al (2020) Polyimide with half encapsulated silver nanoparticles grafted ceramic composite membrane: enhanced silver stability and lasting anti-biofouling performance. *J Memb Sci* 611:118340. <https://doi.org/10.1016/j.memsci.2020.118340>
- Pérez-Vidal A, Rivera-Sanchez SP, Florez-Elvira LJ et al (2019) Removal of *E. coli* and *Salmonella* in pot ceramic filters operating at different filtration rates. *Water Res* 159:358–364. <https://doi.org/10.1016/j.watres.2019.05.028>
- Pottathara YB, Grohens Y, Kokol V et al (2019) Chapter 1 - Synthesis and processing of emerging two-dimensional nanomaterials. In: Beeran Pottathara Y, Thomas S, Kalarikkal N et al (eds) *Micro and nano technologies*. Elsevier, London, pp 1–25
- Rauch KD, MacIsaac SA, Stoddart AK, Gagnon GA (2022) UV disinfection audit of water resource recovery facilities identifies system and matrix limitations. *J Water Process Eng* 50:103167. <https://doi.org/10.1016/j.jwpe.2022.103167>
- Salwan R, Sharma V (2020) Molecular and biotechnological aspects of secondary metabolites in actinobacteria. *Microbiol Res* 231:126374. <https://doi.org/10.1016/j.micres.2019.126374>
- Samaei SM, Gato-Trinidad S, Altaee A (2018) The application of pressure-driven ceramic membrane technology for the treatment of industrial wastewaters: a review. *Sep Purif Technol* 200:198–220. <https://doi.org/10.1016/j.seppur.2018.02.041>
- Sanad MMS, Gaber SE, El-Aswar EI, Farahat MM (2023) Graphene-magnetite functionalized diatomite for efficient removal of organochlorine pesticides from aquatic environment. *J Environ Manage* 330:117145. <https://doi.org/10.1016/j.jenvman.2022.117145>
- Santhosh C, Velmurugan V, Jacob G et al (2016) Role of nanomaterials in water treatment applications: a review. *Chem Eng J* 306:1116–1137. <https://doi.org/10.1016/j.cej.2016.08.053>
- Sha'arani S, Azizan SNF, Md Akhir FN et al (2019) Removal efficiency of gram-positive and gram-negative bacteria using a natural coagulant during coagulation, flocculation, and sedimentation processes. *Water Sci Technol* 80:1787–1795. <https://doi.org/10.2166/wst.2019.433>
- Tamilarasi P, Meena P (2020) Green synthesis of silver nanoparticles (Ag NPs) using *Gomphrena globosa* (Globe amaranth) leaf extract

- and their characterization. *Mater Today Proc* 33:2209–2216. <https://doi.org/10.1016/j.matpr.2020.04.025>
- Tiri RNE, Gulbagca F, Aygun A et al (2022) Biosynthesis of Ag–Pt bimetallic nanoparticles using propolis extract: antibacterial effects and catalytic activity on NaBH₄ hydrolysis. *Environ Res* 206:112622. <https://doi.org/10.1016/j.envres.2021.112622>
- Trang VT, Dinh NX, Lan H et al (2018) APTES functionalized iron oxide-silver magnetic hetero-nanocomposites for selective capture and rapid removal of *Salmonella enteritidis* from aqueous solution. *J Electron Mater* 47:2851–2860. <https://doi.org/10.1007/s11664-018-6135-7>
- Truu M, Ligi T, Nõlvak H et al (2022) Impact of synthetic silver nanoparticles on the biofilm microbial communities and wastewater treatment efficiency in experimental hybrid filter system treating municipal wastewater. *J Hazard Mater* 440:129721. <https://doi.org/10.1016/j.jhazmat.2022.129721>
- Tulinski M, Jurczyk M (2017) Nanomaterials synthesis methods. In: Metrology and standardization of nanotechnology. Wiley, pp. 75–98
- Vijayabharathi R, Sathya A, Gopalakrishnan S (2018) Extracellular biosynthesis of silver nanoparticles using *Streptomyces griseoplanus* SAI-25 and its antifungal activity against *Macrophomina phaseolina*, the charcoal rot pathogen of sorghum. *Biocatal Agric Biotechnol* 14:166–171. <https://doi.org/10.1016/j.bcab.2018.03.006>
- WHO (2021) Silver in drinking water: background document for development of WHO Guidelines for drinking-water quality. World Health Organization, Geneva PP - Geneva
- Yan X, He B, Liu L et al (2018) Antibacterial mechanism of silver nanoparticles in *Pseudomonas aeruginosa*: proteomics approach. *Metallomics* 10:557–564. <https://doi.org/10.1039/c7mt00328e>
- Yang M, Liberatore HK, Zhang X (2019) Current methods for analyzing drinking water disinfection byproducts. *Curr Opin Environ Sci Heal* 7:98–107. <https://doi.org/10.1016/j.coesh.2018.12.006>
- Yu Y, Zhou Z, Huang G et al (2022) Purifying water with silver nanoparticles (AgNPs)-incorporated membranes: recent advancements and critical challenges. *Water Res* 222:118901. <https://doi.org/10.1016/j.watres.2022.118901>
- Zhi X, Mao Y, Yu Z et al (2015) γ -Aminopropyl triethoxysilane functionalized graphene oxide for composites with high dielectric constant and low dielectric loss. *Compos Part A Appl Sci Manuf* 76:194–202. <https://doi.org/10.1016/j.compositesa.2015.05.015>

Publisher's Note Springer Nature remains neutral with regard to jurisdictional claims in published maps and institutional affiliations.